

$U_A(1)$ anomaly and η' mass from an infrared singular quark-gluon vertex

Reinhard Alkofer¹, Christian S. Fischer^{2,3} and Richard Williams²

¹ Graz University, Universitätsplatz 5, A-8010 Graz, Austria

² Institut für Kernphysik, TU Darmstadt, Schlossgartenstrasse 9, 64289 Darmstadt, Germany

³ Gesellschaft für Schwerionenforschung mbH, Planckstr. 1 D-64291 Darmstadt, Germany

September 8, 2008

Abstract. The $U_A(1)$ problem of QCD is inevitably tied to the infrared behaviour of quarks and gluons with its most visible effect being the η' mass. A dimensional argument of Kogut and Susskind showed that the mixing of the pseudoscalar flavour-singlet mesons with gluons can provide a screening of the Goldstone pole in this channel if the full quark-quark interaction is strongly infrared singular as $\sim 1/k^4$. We investigate this idea using previously obtained results for the Landau gauge ghost and gluon propagator, together with recent determinations for the singular behaviour of the quark-gluon vertex. We find that, even with an infrared vanishing gluon propagator, the singular structure of the quark-gluon vertex for certain kinematics is apposite for yielding a non-zero screening mass.

PACS. 11.30.Rd – 11.30.Fs – 12.38.Lg – 14.40.Aq

1 Generalities on the $U_A(1)$ Anomaly

It has now been long accepted that the strong interaction is described by a Yang-Mills theory, whose non-Abelian character exhibits the properties of asymptotic freedom and confinement. However, despite our accedence to this we still have no satisfactory understanding of the confinement phenomena itself. It is envisaged that it is in the infrared structure of QCD where this mechanism lies, and so we must probe in a momentum region characterised by large values of the coupling. Here, standard tools such as perturbation theory are inapplicable and lattice calculations typically use volumes too small to reliably probe the deep infrared.

The idea of ‘infrared slavery’ gave rise to two possible behaviours for the strong running coupling at small momenta [1]: either it exhibits an IR fixed point or diverges at the origin. From functional methods in Landau gauge it is the former behaviour that seems likely in the Yang-Mills sector [2, 3, 4, 5, 6]. However, such a fixed point behaviour of the coupling does not predicate that the vertex functions themselves are infrared finite. Indeed, depending upon the number of external ghost and gluon legs, many 1PI Green’s functions are found to be singular in the infrared [5, 6, 7]. For the quark-gluon vertex, this issue is addressed in [8]. In this paper it is our aim to address yet another puzzle of QCD, with the infrared behaviour of the quark-gluon vertex playing a crucial rôle.

We know that the up and down quark are very light, and so may consider them massless to good approximation. To a lesser extent, the same may be assumed for the strange quark and so we expect the Lagrangian of QCD to exhibit an approximate $SU(N_f) \times SU(N_f)$ symmetry, with $N_f = 3$. Assuming the

chiral limit is realised, this is broken dynamically to a diagonal $SU_V(3)$, and so gives rise to eight Goldstone bosons.

However, we also expect the same mechanism to break the $U_A(1)$ symmetry of the QCD Lagrangian. Thus one should find a ninth isosinglet pseudoscalar boson corresponding to the spontaneous breaking of this symmetry. However, on examining the spectrum of observed mesons this proves to be one Nambu-Goldstone boson too many. The lightest candidate for this is the η' , whose mass of $m_{\eta'} \sim 958$ MeV is far from being ‘light’. In fact, it has been shown that if the $U_A(1)$ symmetry is not explicitly broken, then the mass of the η' must be less than $\sqrt{3}m_\pi \sim 250$ MeV [9]. Even allowing for the mass of the strange quark, the η' remains far too heavy to be solely described in this manner. This is the $U(1)$ problem of QCD.

A step towards resolution came from the recognition that the classical $U_A(1)$ symmetry is anomalous, *i.e.* broken by quantum mechanical effects. However, it is found that the associated current is a total divergence, and hence no symmetry breaking contribution is obtained for *finite* order in perturbation theory [10]. Thus, the mechanism of the anomalous breaking of the $U_A(1)$ symmetry must be wholly non-perturbative in nature.

There have been several suggestions as to how the η' obtains its unexpectedly large mass. In the early days of QCD Kogut and Susskind pointed out, on dimensional grounds, that a contribution to the η' in the chiral limit could be obtained by the mixing between two infrared enhanced gluons, with momentum space propagator $D(k) \sim 1/k^4$ for $k^2 \rightarrow 0$ [11]. A few years later topological solutions termed *instantons* were discovered in QCD [12]. In contradistinction to the confinement driven Kogut-Susskind scenario, these gave rise to an al-

ternative solution of the $U_A(1)$ problem: Instantons were shown by 't Hooft to lead to the non-conservation of the axial charge and so induce a $2N_f$ fermion operator giving rise to a non-zero η' -mass in the chiral limit [13, 14]. Again a few years later Witten and Veneziano [15, 16, 17] proposed their solution of the problem by considering an expansion of QCD in N_f/N_c , where N_f and N_c are the number of flavours and colours respectively. They showed that the correct pattern of the $U_A(1)$ -symmetry breaking can be obtained if the anomalous mass of the η' is related to the topological susceptibility of the theory. Since this susceptibility is not necessarily generated by instantons Veneziano named his paper ‘ $U(1)$ without instantons’ [16]. Indeed, a different type of topologically non-trivial gluon field configurations leading to a non-vanishing topological susceptibility are center vortices as *e.g.* discussed in ref. [18].

Certainly, with the Witten-Veneziano mechanism at hand confinement and topology based explanations for the $U_A(1)$ anomaly are not mutually exclusive. The reason is simply that well-established suggestions for topology driven mechanisms for confinement exist [50]. Thus the same topologically non-trivial gauge field configurations could be responsible for both confinement and the resolution of the $U_A(1)$ -problem.

In this letter we concern ourselves with the Kogut-Susskind mechanism employing an approach similar to that given in [19, 20]. We employ solutions to the Dyson-Schwinger equations for the propagators of QCD and the quark-gluon vertex to determine the anomalous mass of the η' in the chiral limit. The technical details are discussed in sections 2 - 4. We present our result in section 5 and discuss its relation to the Witten-Veneziano mechanism in section 6. We summarise in section 7. We wish to note that all calculations are done in Euclidean momentum space. Furthermore, we will ignore all effects from isospin breaking and work in the isospin limit.

2 Flavour mixing

A suitable basis to describe the flavour content of mesons is given by the $SU(3)$ singlet and octet basis:

$$\begin{aligned} |\pi^0\rangle &= (|u\bar{u}\rangle - |d\bar{d}\rangle) / \sqrt{2} \\ |\eta_8\rangle &= (|u\bar{u}\rangle + |d\bar{d}\rangle - 2|s\bar{s}\rangle) / \sqrt{6} \\ |\eta_0\rangle &= (|u\bar{u}\rangle + |d\bar{d}\rangle + |s\bar{s}\rangle) / \sqrt{3} \end{aligned} \quad (1)$$

The octet-singlet mass squared matrix in the isospin limit is thus given by

$$M^2 = \begin{pmatrix} M_\pi^2 & 0 & 0 \\ 0 & M_{88}^2 & M_{80}^2 \\ 0 & M_{08}^2 & M_{00}^2 + m_A^2 \end{pmatrix}, \quad (2)$$

with matrix elements

$$\begin{aligned} M_{88}^2 &= \frac{2}{3} (m_{s\bar{s}}^2 + \frac{1}{2}m_\pi^2) = \frac{1}{3} (4m_K^2 - m_\pi^2) \\ M_{80}^2 = M_{08}^2 &= \frac{\sqrt{2}}{3} (m_\pi^2 - m_{s\bar{s}}^2) = \frac{2\sqrt{2}}{3} (m_\pi^2 - m_K^2) \\ M_{00}^2 &= \frac{2}{3} (\frac{1}{2}m_{s\bar{s}}^2 + m_\pi^2) = \frac{1}{3} (2m_K^2 + m_\pi^2). \end{aligned} \quad (3)$$

Here, we have employed $m_{s\bar{s}} = 2m_K^2 - m_\pi^2$ from the Gell-Mann-Oakes-Renner relation to make the substitution on the right-hand side. With the basis of (1) the pion is decoupled in the isospin limit. Thus we concentrate on the 2×2 sub-matrix that mixes the η and η' [16]:

$$\frac{1}{3} \begin{pmatrix} 4m_K^2 - m_\pi^2 & 2\sqrt{2}(m_\pi^2 - m_K^2) \\ 2\sqrt{2}(m_\pi^2 - m_K^2) & 2m_K^2 + m_\pi^2 + 3m_A^2 \end{pmatrix}. \quad (4)$$

The anomalous mass term, m_A^2 is related to the topological susceptibility χ^2 through the Witten-Veneziano formula [15, 16, 17]

$$m_A^2 = 2 \frac{N_f}{f_0^2} \chi^2, \quad (5)$$

which includes the pion decay constant $f_0 \simeq 93\text{MeV}$. By now its derivation has been refined and it has been adapted to lattice gauge theory and found to nicely agree with theoretical expectations and experimental data [21, 22, 23, 24, 25], with values reported of the order $\chi^2 \sim (191 \pm 5 \text{MeV})^4$. It is important to note, however, that the corresponding Witten-Veneziano mechanism does not make any reference as to which degrees of freedom are responsible for the generation of χ^2 . We come back to this point in section 6.

The η_0 and η_8 are not the physical mass eigenstates, and so we diagonalise the 2×2 mass-matrix by introducing the following unitary transformation:

$$(\eta \ \eta') = \begin{pmatrix} \cos \theta & -\sin \theta \\ \sin \theta & \cos \theta \end{pmatrix} \begin{pmatrix} \eta_8 \\ \eta_0 \end{pmatrix}. \quad (6)$$

with θ the singlet-octet mixing angle. This gives rise to the following mass eigenstates:

$$m_\pm^2 = m_K^2 + \frac{m_A^2}{2} \pm \Delta, \quad (7)$$

with m_+ , m_- corresponding to the η' and η respectively, and the shift Δ given by:

$$\Delta = \sqrt{(m_K^2 - m_\pi^2)^2 - \frac{m_A^2}{3} (m_K^2 - m_\pi^2) + \frac{m_A^4}{4}}. \quad (8)$$

A phenomenological value for the mixing angle can be calculated from:

$$\tan \theta = -\frac{1}{2\sqrt{2}} \left[1 - \frac{3}{m_K^2 - m_\pi^2} \left(\frac{m_A^2}{2} - \Delta \right) \right], \quad (9)$$

with the current values $m_K = 498 \text{MeV}$, $m_\pi = 135 \text{MeV}$ [26]. Here, the required input is the anomalous mass contribution m_A^2 . The Random Instanton Liquid Model provides a mixing angle of $\theta \simeq -11.5^\circ$ [27, 28], whilst knowledge of the η and η' masses, respectively about 547 and 958MeV, suggests $\sim -20^\circ$. A detailed study of the available observables yields an average value of -15.4° [29].

3 Anomalous Contribution of the Gluon

If we ignore the contribution from the gluon anomaly, that is by setting $m_A^2 = 0$, we would expect the flavour content of our η ,

η' to be analogous to that of the ω , ρ system where ideal mixing is realised to very good approximation. Diagonalising (2) entails that the mass of the eta be degenerate with that of the pion, with flavour content $(u\bar{u} + d\bar{d})/\sqrt{2}$, whilst the η' would be a pure $s\bar{s}$ pseudoscalar. We know this to be far from the truth since this would provide a mixing of $\theta \simeq -54.7^\circ$, hence the $U_A(1)$ -problem and the desire to include anomalous contributions from the gluon.

To do so in the Dyson-Schwinger and Bethe-Salpeter approach is a formidable task, for presently we are limited by kernels that include only re-summations of gluon ladders. These do not include the necessary annihilation (and consequent re-combination) of $q\bar{q}$ pseudoscalar meson into two gluons. Typically, the $U_A(1)$ -breaking term is put in by hand and adjusted as a free parameter to obtain phenomenological results.

The minimal diagram that includes the gluon Adler-Bell-Jackiw (ABJ) diagram is given in fig. 1. We later comment upon the contribution of diagrams with more than two gluon exchange.

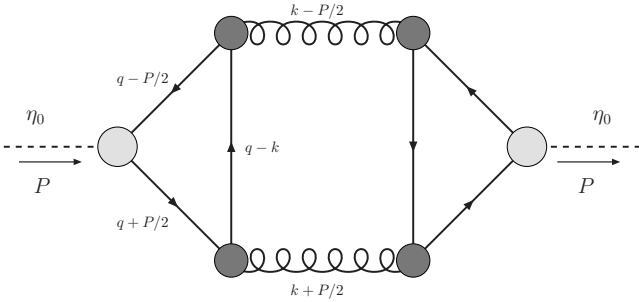


Fig. 1. The diamond diagram $\Pi(P^2)$. The crossed gluon exchange contribution gives rise to an additional factor of two.

For a simple model, Kogut and Susskind gave arguments as to how a non-vanishing contribution to the η' -mass in the chiral limit could be obtained [11]. This has been explored phenomenologically in a previous study [19,20], in order to gauge the magnitude of the effect should it be realised. There, an ansatz for the gluon propagator has been employed which is infrared singular supplemented by a perturbative tail. Though such a form cannot naturally arise from consideration of gluons alone, at the time there were already suggestions that in Landau gauge the ghost sector was strongly infrared enhanced and could thus enter into the effective gluon propagator implicitly. Using parameters given in that paper, a screening-mass squared of about half the required amount is obtained, giving credence to the mechanism. However, nothing definitive may be claimed until dressed Green's functions are employed, whose behaviour is well-founded in the infrared.

In order to move beyond this qualitative study, we use explicit calculations for the gluon obtained in previous calculations [31,32]. Since these prove to be infrared vanishing, it is important that we have a self-consistent and motivated dressing for the quark-gluon vertex that compensates for this precisely, again leading to a non-vanishing topological susceptibility in the chiral limit. Our starting point for the calculation is the diagram shown in fig. 1. It consists of two anomalous AVV tri-

angle diagrams [33], which here are obviously non-Abelian in nature [13]. These triangles are linked via the exchange of two gluons. Note that should we exchange three gluons or more in the t -channel, one would couple in a pseudoscalar $J^{PC} = 0^{-+}$ glueball, whose large mass of ~ 2 GeV [34] would heavily suppress the contribution. For multiple gluon exchange in the s -channel, however we essentially re-sum a gluon ladder which is related to meson exchange [35]. For this, the scalar part of the vertex which we have neglected to model here is important.

Staying with two-gluon exchange and thus restricting ourselves to a qualitative study, we write the amplitude of fig. 1 explicitly as an integral over the gluon momenta:

$$\Pi(P^2) = \int \widetilde{d}k G_{\mu\rho}^{ac}(P, k) D_{ab}^{\mu\nu}(k_+) D_{dc}^{\rho\sigma}(k_-) G_{\sigma\nu}^{db}(-P, k), \quad (10)$$

with $\widetilde{d}k$ shorthand for the invariant measure $d^4k/(2\pi)^4$, and $k_{\pm} = k \pm P/2$. We have chosen an equal momentum partition to simplify the resulting equations; the final result should be independent of this choice. The quark triangle, $G_{\mu\nu}^{ab}$, arising from the axial anomaly is:

$$G_{\mu\nu}^{ab}(P, k) = g^2 \int \widetilde{d}q \left\{ \text{tr} \left[\Gamma_{\eta}(P, q) S(q_+) \Gamma_{\mu}^a(q_+, q-k) \right. \right. \\ \times S(q-k) \Gamma_{\nu}^b(q_-, q-k) S(q_-) \left. \right] \\ + \text{tr} \left[\Gamma_{\eta}(P, q) S(q_+) \Gamma_{\nu}^b(q_+, q+k) \right. \\ \left. \left. \times S(q+k) \Gamma_{\mu}^a(q_-, q+k) S(q_-) \right] \right\}, \quad (11)$$

where the trace is over Dirac and colour indices, and the second term accounts for the crossed gluon-exchange. Solution of this equation requires knowledge of the pseudoscalar Bethe-Salpeter amplitude (BSA) for the $\Gamma_{\eta}(P, k)$, the full quark propagator $S(k)$, and the quark-gluon vertex $\Gamma_{\mu}^a(k, q)$.

4 Computational Inputs

To calculate the quantities required for computation of the diamond diagram, we employ the Dyson-Schwinger approach to QCD, see [36,37,38,39] for reviews. These comprise of an infinite tower of coupled integral equations that interrelate the fundamental Green's functions of the theory. Despite analytic studies being possible in certain kinematical situations [3,5,6,40,7], in principle one must employ a truncation scheme and perform the calculations numerically. In the present context it is, however, important to mention that anomalous diagrams are represented exactly if the underlying symmetries are respected, see *e.g.* refs. [41,42].

4.1 Yang-Mills Propagators

The pure Yang-Mills (YM) sector of QCD is comprised of both ghosts and gluons, whose propagators in Euclidean space are

written:

$$D^G(p^2) = -\frac{G(p^2)}{p^2}, \quad D_{\mu\nu}^{ab} = \delta^{ab} \left(\delta_{\mu\nu} - \frac{p_\mu p_\nu}{p^2} \right) \frac{Z(p^2)}{p^2}. \quad (12)$$

where $G(p^2)$ and $Z(p^2)$ are the ghost and gluon dressing functions respectively. These satisfy the Dyson-Schwinger equations shown pictorially in fig. 2, and have been studied in Landau gauge by employing truncations at the level of the vertices. It is found that in the infrared these can be described by power laws [2, 3, 44]:

$$G(p^2) \sim (p^2)^{-\kappa}, \quad Z(p^2) \sim (p^2)^{2\kappa}, \quad (13)$$

with κ a positive constant, giving rise to an infrared diverging ghost propagator and vanishing gluon. Moreover, with a bare ghost-gluon vertex one finds $\kappa = (93 - \sqrt{1201})/98 \simeq 0.595$, and so we see IR dominance of the ghost in Landau gauge. This fact greatly affects our calculation of (10) since we now entirely depend upon the dressing of the quark-gluon vertex to yield the sufficient infrared enhancement that will lead to non-vanishing $\Pi(P^2 \rightarrow 0)$.

From the ghost-gluon vertex we may define the running coupling:

$$\alpha(p^2) = \alpha_\mu G^2(p^2) Z(p^2), \quad (14)$$

which may be parameterised such that the numerical results for Euclidean scales are accurately reproduced [32]:

$$\alpha_{\text{fit}}(p^2) = \frac{\alpha_s(0)}{1 + p^2/\Lambda_{\text{QCD}}^2} + \frac{4\pi}{\beta_0} \frac{p^2}{\Lambda_{\text{QCD}}^2 + p^2} \times \left(\frac{1}{\ln(p^2/\Lambda_{\text{QCD}}^2)} - \frac{1}{p^2/\Lambda_{\text{QCD}}^2 - 1} \right). \quad (15)$$

Here $\beta_0 = (11N_c - 2N_f)/3$, and $\alpha_S(0)$ is the fixed point in the infrared, calculated to be $8.915/N_c$ for our choice of κ .

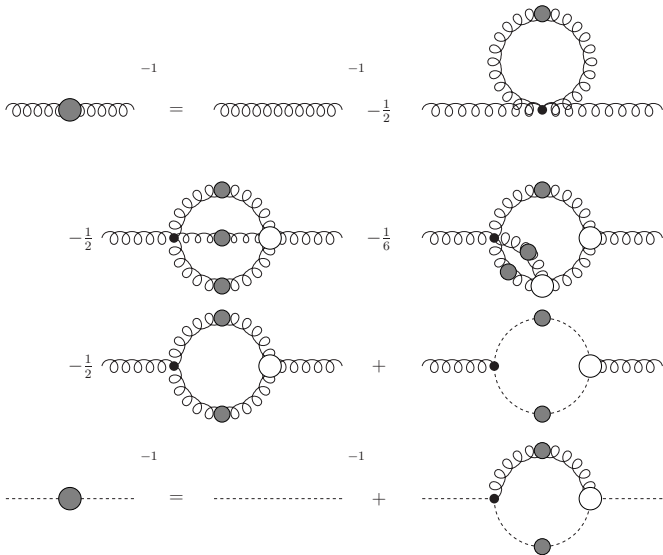


Fig. 2. The gluon and ghost Dyson-Schwinger equation. Filled blobs indicate dressed propagators and vertices.

Similarly, the gluon dressing function may be fitted [32]:

$$Z(k^2) = \left(\frac{k^2}{k^2 + \Lambda_{\text{QCD}}^2} \right)^{2\kappa} \left(\frac{\alpha_{\text{fit}}(k^2)}{\alpha_\mu} \right)^{-\gamma}, \quad (16)$$

such that no further singularities are introduced. Here, $\gamma = (-13N_c + 4N_f)/(22N_c - 4N_f)$ is the one-loop value for the anomalous dimension of the gluon propagator, and $\alpha_\mu = 0.2$ at the renormalisation scale $\mu^2 = 170 \text{ GeV}^2$. We use $\Lambda_{\text{QCD}}^2 = 0.5 \text{ GeV}^2$ similar to the scale obtained in ref. [32].

4.2 The Gap Equation

A far simpler system to that of the Yang-Mills sector, though one of equal if not greater importance, is that for the quark propagator, shown in fig. 3. This may be written explicitly:

$$S^{-1}(p) = Z_2 [S^{(0)}(p)]^{-1} - C_F \frac{\tilde{Z}_1 Z_2}{\tilde{Z}_3} \frac{g^2}{(2\pi)^4} \int d^4 k \gamma_\mu S(k) \Gamma_\nu(k, p) D_{\mu\nu}(p - k). \quad (17)$$

As is evident, this is a non-linear equation dependent upon the form of the quark propagator itself, the gluon propagator and a higher order Green's function, the quark-gluon vertex $\Gamma_\nu(k, p)$. The quark propagator consists of a Dirac-odd and Dirac-even part, and so is completely described by two momentum dependent functions:

$$S(p) = \frac{i\not{p} + M(p^2)}{p^2 + M^2(p^2)} Z_f(p^2), \quad (18)$$

with $M(p^2)$ the mass function and $Z_f(p^2)$ the wave-function renormalisation, which are both assumed to be non-singular in the infrared. This behaviour is indeed what is seen in numerical calculations [31, 8]. In the following we consider the quarks in the chiral limit, i.e. $[S^{(0)}(p)]^{-1} = i\not{p}$. Then $M(p^2)$ only contains effects from the dynamical breaking of chiral symmetry and in the $\eta - \eta'$ -mixing we only have the contribution m_A from the topological susceptibility (5).

4.3 Quark-Gluon Vertex

Earlier we stated that in light of the vanishing nature of the gluon propagator in the deep IR, it is the behaviour of the quark-gluon vertex there that is crucial.



Fig. 3. The quark Dyson-Schwinger equation. Filled blobs indicate dressed propagators and vertices.

4.3.1 Vertex for all scales vanishing

From the IR analysis of [40, 8] we know that the quark-gluon vertex, $\Gamma_\mu^a = \frac{\lambda^a}{2} \Gamma_\mu$, should have the behaviour:

$$\Gamma \sim (\bar{p}^2)^{-\kappa-1/2}, \quad (19)$$

when the sum of all incoming momenta, \bar{p} , are vanishing in the infrared; that is, it is strongly infrared enhanced. They find that all twelve possible structures of the quark-gluon vertex may contribute in the infrared, with vector and scalar pieces playing a dominant rôle. Thus one may parameterise Γ_ν by:

$$\Gamma_\nu(p, q) = L_1(p, q) \gamma_\nu - i L_3(p, q) (p + q)_\nu \quad (20)$$

with p and q the incoming and outgoing quark momenta respectively, and $k = p - q$ the outgoing gluon momentum.

We wish to find a non-vanishing $\Pi(P^2 \rightarrow 0)$, and thus look at the quark-triangle $G_{\mu\nu}^{ab}$ in the limit of the incident gluon momenta vanishing, i.e. $k, P \ll \Lambda_{\text{QCD}}$. We note that we may write:

$$G_{\mu\nu}^{ab} = \frac{1}{2} \delta^{ab} \epsilon_{\mu\nu\alpha\beta} P^\alpha k^\beta I(P^2, k^2, k \cdot P), \quad (21)$$

where I represents the internal loop integral of the quarks, obtained by separating out the tensor structure. We then evaluate the behaviour of I numerically, using the power laws (13) and (19) for the gluon propagator and the quark-gluon vertex, respectively, and an infrared finite quark propagator and Bethe-Salpeter amplitude. We then find that the dominant infrared behaviour of the triangle is given by:

$$I(P^2, 0, 0) \sim (P^2)^{-2\kappa+1}. \quad (22)$$

On dimensional grounds this behaviour is insufficient to generate $\Pi \neq 0$ in the limit $P^2 \rightarrow 0$. We thus conclude that the uniform scaling behaviour (19) of the quark-gluon vertex is not sufficient to account for the Kogut-Susskind mechanism.

4.3.2 Soft Singularity

However, there is not just one momentum configuration giving rise to a singular structure in the vertex. There also exists a soft collinear-like divergence dependent only upon the external gluon momentum k^2 :

$$\Gamma \sim (k^2)^{-\kappa-1/2} \quad (23)$$

This additional divergence has been identified from the Dyson-Schwinger equation for the quark-gluon vertex in ref. [8]. Its appearance in the quark-antiquark scattering kernel for heavy quarks leads to a linearly rising potential and consequently to quark-confinement. Since the derivation of eq. (23) is somewhat involved we do not wish to repeat it here but instead refer the interested reader directly to ref. [8].

For the integrand I at small momenta this soft divergence leads to

$$I(P^2, 0, 0) \sim (P^2)^{-2\kappa-1}, \quad (24)$$

a behaviour which we have obtained both by analytical power counting and also numerically. To gauge the impact of this result on our evaluation of $\Pi(P^2 \rightarrow 0)$, we insert (21) into (10) to obtain:

$$\Pi(P^2) = 64 \int \widetilde{dk} (k \cdot P)^2 \frac{Z(k_+^2)}{k_+^2} \frac{Z(k_-^2)}{k_-^2} I^2. \quad (25)$$

A simple check of the dimensions indicates that a non-zero contribution to the anomalous mass is obtained. Only the magnitude of this needs now be determined. To this end, we must still determine the Bethe-Salpeter amplitude for the η .

4.4 The Bethe-Salpeter equation

An essential input to the diamond diagram is the Bethe-Salpeter amplitude for the η . This can be obtained by solving the pseudoscalar Bethe-Salpeter equation (BSE), which describes $q\bar{q}$ bound-states:

$$\Gamma_{tu}(p; P) = \int \widetilde{dk} K_{tu;rs}^{YM}(p, k; P) [S(k_+) \Gamma(k; P) S(k_-)]_{sr}, \quad (26)$$

where K represents the (unknown) quark-antiquark scattering kernel, $k_+ = k + \eta P$, $k_- = k + (\eta - 1)P$, η is the momentum partitioning of the quarks. The meson has total momentum P , taken in the rest frame, with $P^2 = -m^2$ and m the mass of the bound-state.

Fundamental to any study of pseudoscalar mesons is the axial-vector Ward-Takahashi identity (AV-WTI):

$$P_\mu \Gamma_{5\mu}^a(k; P) = S^{-1}(k_+) \frac{1}{2} \lambda_f^a i \gamma_5 + \frac{1}{2} \lambda_f^a i \gamma_5 S^{-1}(k_-) - M_\zeta i \Gamma_5^a(k; P) - i \Gamma_5^a(k; P) M_\zeta. \quad (27)$$

Since the left-hand side involves the BSE, whilst the right-hand side involves the quark SDE, a non-trivial relationship between the kernels is established. Thus one must treat the Bethe-Salpeter kernel K and the quark-gluon vertex in such a way that the AV-WTI is satisfied, otherwise a massless pion will not be found in the chiral limit. A generalisation of this identity to the case of the flavour singlet channel has been given in ref. [43]. A suitable truncation scheme used frequently [38] is the rainbow-ladder approximation which we also employ here.

4.5 Phenomenologically qualitative model

In rainbow-ladder approximation the quark-gluon vertex is restricted to its γ_ν part. We therefore simplify the parametrisation (20) further and write:

$$\Gamma_\nu(k, p) = Z_{1F}(\mu^2, \Lambda^2) L_1(k^2, \mu^2) \gamma_\nu. \quad (28)$$

Here the vertex renormalisation constant Z_{1F} provides multiplicative renormalisability of the vertex and also of the resulting quark SDE and pseudoscalar BSE. The vertex dressing L_1 is parameterised by:

$$L_1(z) = \left(\frac{z}{z + d_2} \right)^{-1/2-\kappa} \left(\frac{d_1}{1 + z/d_2} + \frac{z d_3}{d_2^2 + (z - d_2)^2} \right)$$

$$+ \frac{z}{d_2 + z} \left[\frac{4\pi}{\beta_0 \alpha_\mu} \left(\frac{1}{\log(z/d_2)} - \frac{d_2}{z - d_2} \right) \right]^{-2\delta} \quad (29)$$

with $z = k^2$ the gluon momentum and d_1 sets the strength of the interaction in the infrared. The scale d_2 is set to $d_2 = (0.5\text{GeV})^2 \approx \Lambda_{\text{QCD}}^2$, i.e. similar to the scale found in the Yang-Mills-sector. The parameter d_3 determines the size of a term added to give additional integrated strength in the intermediate momentum regions.

This construction is necessary to produce meaningful results: Since the AV-WTI forces us at present to only consider the γ_μ -part of the quark-gluon interaction we necessarily miss some interaction strength in the intermediate momentum region. This cannot be compensated for by an increase of d_1 as discussed in the following.

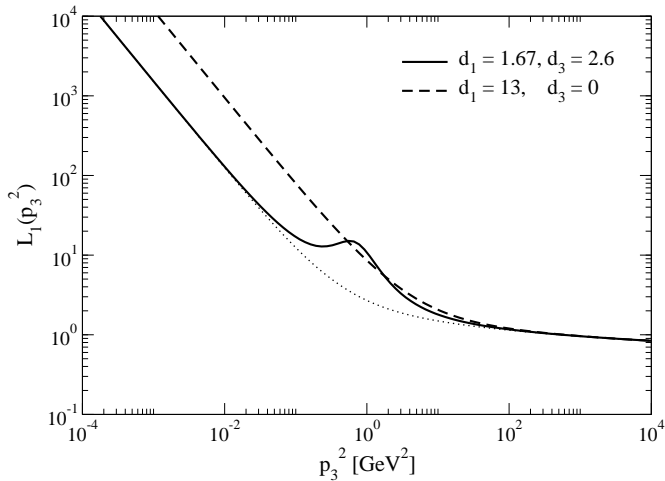


Fig. 4. Our model dressing for the γ^μ part of the vertex. See the text for a description of each.

In fig. 4 we plot two examples of L_1 . The parameters of the dashed line have been fitted such that the physical masses of the π and the ρ are reproduced, employing d_1 and d_2 only. Here we need a large value of $d_1 = 13$, which leads to an extremely strong infrared singularity; employing such a form in the diamond diagram would yield results for the topological mass m_A^2 which are orders of magnitudes too large to account for the experimental η and η' -masses. To account for this, we introduce extra interaction strength in the intermediate momentum region parameterised by d_3 . This additional bump generates correct π and ρ -masses whilst allowing for a reduction of the infrared scale d_1 to a realistic order. Note, that this particular shape and strength of interaction is also suggested by the results for the running coupling of the quark-gluon vertex, found in [8].

Once our parameters are fixed, we obtain solutions for the Bethe-Salpeter amplitude in the chiral limit, which are then employed in the calculation of the diamond diagram.

5 Results

Naïvely, the diamond diagram consists of a twelve dimensional integral which can be reduced to eight dimensions by symmetry considerations. In the limit $P^2 \rightarrow 0$ the integrand simplifies further and the problem may be reduced to a five dimensional integral. We solved this integral both, by Monte-Carlo techniques and using adaptive quadrature routines and found the latter method to be superior. Sufficient accuracy of the order of one percent is obtained within a few minutes of CPU-time.

In table 1 we give our results for the calculation of the diamond diagram shown in fig. 1, employing the model of the quark-gluon interaction discussed above. Within the limitations of the model we may not expect quantitatively correct results. Nevertheless we obtain reasonable values for the masses and the mixing angle at least for the last parameter set considered. For this set, we find a topological susceptibility,

$$\chi^2 = (169 \text{ MeV})^4, \quad (30)$$

in qualitative agreement with lattice results [25]. Qualitatively we do see that it is precisely the infrared collinear behaviour of the quark-gluon vertex that is necessary to obtain a non-zero contribution to the topological susceptibility.

A quantitative study would require a self-consistent solution for the quark-gluon vertex employing fewer approximations. Then, at least in the $P^2 \rightarrow 0$ limit, one need not solve the pseudoscalar BSE since the leading term $\gamma_5 B(q^2)/f_\pi$ in chiral limit is known from the quark DSE. We would then need to consider higher-order diagrams corresponding to the diamond diagram, with n -gluon exchange taking place in the s -channel. This ladder re-summation of gluons is often represented by a single meson exchange. This picture has been explored in ref. [35] as a means of generating the topological mass of the η' . However, since the actual mechanism of anomalous $U_A(1)$ symmetry breaking may not be explained in terms of gauge independent particle exchange, such as a pion, this picture cannot be entirely adequate.

6 Discussion of topological effects and infrared singularities

As we have seen the infrared divergence of the quark-gluon vertex plays an important rôle in a confinement-based explanation of the η' mass and thus the $U_A(1)$ anomaly. On the other hand, it is evident that the η' mass is linked to the topological susceptibility via the Witten-Veneziano formula (5) and thus topologically non-trivial gluon field configurations. How can such a dichotomy be resolved?

In a first step to a potential solution of this puzzle we note that it is not only instantons that are capable of providing a non-vanishing topological susceptibility. As a matter of fact, there is evidence [45, 46, 47] that on the lattice, field configurations with non-trivial holonomy have been misidentified as instantons. They are more like Kraan-van-Baal-Lee-Lu calorons [48, 49] than instantons. And, amongst these and other topologically non-trivial gluon field configurations, also center vortices (see *e.g.* the reviews [50]) provide a non-vanishing topological

d_1 GeV ²	d_2 GeV ²	d_3 GeV ²	m_π MeV	m_ρ MeV	m_A^2 GeV ²	χ^2 (MeV) ⁴	θ	m_η MeV	$m_{\eta'}$ MeV
1.41	0.5	2.6	135	735	0.30	144	-35.3	412	790
1.55	0.5	2.6	135	741	0.48	162	-29.1	450	840
1.67	0.5	2.6	135	747	0.56	169	-23.2	479	906

Table 1. Numerical results of the calculation of the diamond diagram for a range of parameters. The π and ρ phenomenology is only marginally affected by these small changes in infrared strength, yet note the strong effect on the calculated anomalous mass.

susceptibility [18,51]. At least, for these latter field configurations we know that they provide an explanation for quark confinement [50,52], and that in most gauges, including the Landau gauge, a substantial amount of these configurations live on the Gribov horizon. The latter property is responsible that, when removing center vortices from a lattice ensemble, not only the string tension vanishes but also the Landau gauge ghost propagator becomes infrared finite [53].

In the confinement based scenario described within this letter, the infrared divergence of the quark-gluon vertex is the cause for the η' mass. It is driven by the infrared divergence of the three-gluon gluon vertex and thus eventually by the infrared behaviour of the ghost propagator [40]. In Landau gauge (as well as in some other gauges) this infrared divergence is, according to the Gribov-Zwanziger scenario, assumed to be caused by the dominance of field configurations on the Gribov horizon (or, more precisely, on the non-vanishing overlap of the boundary of the fundamental modular region with the Gribov horizon). At least, some of these field configurations, as *e.g.* the center vortices, are topologically non-trivial. If the Gribov-Zwanziger scenario is correct they provide confinement. But they may also provide a non-vanishing topological susceptibility and thus the $U_A(1)$ anomaly, especially the η' mass. When using, instead of a lattice Monte-Carlo calculation, a functional approach (as Dyson-Schwinger or Renormalization Group Equations) topological effects are encoded in the infrared behaviour of the Green functions. In Landau gauge it is the chain of infrared divergences of the ghost propagator, the three-gluon and the quark-gluon vertex which seems to be responsible for both, confinement and the $U_A(1)$ anomaly. This is, however, only a reflection of the fact that certain types of gluon field configurations cause both, confinement and the $U_A(1)$ anomaly.

If one is willing to accept this scenario a further conclusion is evident: the $U_A(1)$ -relevant, topologically non-trivial gluon field configurations are intimately related to confinement, and thus are very likely not the instantons discovered already more than thirty years ago [12]. In addition, we know at least one type of gluon field configuration satisfying the requirements of this scenario, namely center vortices. However, at this point the relevance of other configurations to confinement and the $U_A(1)$ anomaly cannot be excluded.

7 Summary

We investigated the Kogut-Susskind mechanism for the resolution of the $U_A(1)$ problem of QCD, employing known results for the ghost and gluon propagators from Landau gauge studies of the Yang-Mills sector, together with recent results for

the quark-gluon vertex. Taking the qualitative features of this study, we modelled the vertex-dressing such that an infrared soft-singularity was present, whilst at the same time matching meson observables for the π and the ρ . The presence of a collinear singularity [8], dominant in the gluon momentum, proves essential to the generation of a non-zero topological susceptibility in the chiral limit, as required by the Witten-Veneziano mechanism. Our study illustrates the effects of topologically non-trivial field configurations on the level of correlation functions and therefore provides a qualitatively feasible mechanism for the resolution of the mass of the η' in a functional approach to QCD.

Acknowledgements

We are grateful to Felipe Llanes-Estrada, Craig Roberts, Kai Schwenzer and Lorenz von Smekal for fruitful discussions on this problem. RW thanks the hospitality of Graz where much of this work was undertaken. RA and RW have been supported by the Deutsche Forschungsgemeinschaft (DFG) under Grant No. A1279/5-2, CF and RW have been supported by the Helmholtz-University Young Investigator Grant VH-NG-332.

References

1. S. Weinberg, Phys. Rev. Lett. **31** (1973) 494; D. J. Gross and F. Wilczek, Phys. Rev. D **8** (1973) 3633.
2. L. von Smekal, R. Alkofer and A. Hauck, Phys. Rev. Lett. **79** (1997) 3591 [arXiv:hep-ph/9705242].
3. C. Lerche and L. von Smekal, Phys. Rev. D **65** (2002) 125006 [arXiv:hep-ph/0202194].
4. J. M. Pawłowski, D. F. Litim, S. Nedelko and L. von Smekal, Phys. Rev. Lett. **93** (2004) 152002 [arXiv:hep-th/0312324].
5. R. Alkofer, C. S. Fischer and F. J. Llanes-Estrada, Phys. Lett. B **611** (2005) 279 [arXiv:hep-th/0412330].
6. C. S. Fischer and J. M. Pawłowski, Phys. Rev. D **75** (2007) 025012 [arXiv:hep-th/0609009].
7. R. Alkofer, M. Q. Huber and K. Schwenzer, arXiv:0801.2762 [hep-th].
8. R. Alkofer, C. S. Fischer, F. J. Llanes-Estrada and K. Schwenzer, Annals of Physics, in press; arXiv:0804.3042 [hep-ph].
9. S. Weinberg, Phys. Rev. D **11** (1975) 3583.
10. H. Fritzsch, M. Gell-Mann and H. Leutwyler, Phys. Lett. B **47** (1973) 365.
11. J. B. Kogut and L. Susskind, Phys. Rev. D **10** (1974) 3468.
12. A. A. Belavin, A. M. Polyakov, A. S. Shvarts and Yu. S. Tyupkin, Phys. Lett. B **59** (1975) 85.
13. G. 't Hooft, Phys. Rev. Lett. **37** (1976) 8.
14. G. 't Hooft, Phys. Rept. **142** (1986) 357.

15. E. Witten, Nucl. Phys. B **156** (1979) 269.
16. G. Veneziano, Nucl. Phys. B **159** (1979) 213; P. Di Vecchia and G. Veneziano, Nucl. Phys. B **171** (1980) 253.
17. G. Veneziano, Phys. Lett. B **95** (1980) 90.
18. M. Engelhardt, Nucl. Phys. B **585** (2000) 614 [arXiv:hep-lat/0004013].
19. L. von Smekal, A. Mecke and R. Alkofer, arXiv:hep-ph/9707210.
20. A. Mecke, Diploma thesis, University of Tübingen, 1997.
21. E. Seiler and I. O. Stamatescu, preprint MPI-PAE/PTH10/87; E. Seiler, Phys. Lett. B **525** (2002) 355 [arXiv:hep-th/0111125].
22. L. Giusti, G. C. Rossi, M. Testa and G. Veneziano, Nucl. Phys. B **628** (2002) 234 [arXiv:hep-lat/0108009].
23. L. Giusti, G. C. Rossi and M. Testa, Phys. Lett. B **587** (2004) 157 [arXiv:hep-lat/0402027].
24. M. Luscher, Phys. Lett. B **593**, 296 (2004) [arXiv:hep-th/0404034].
25. L. Del Debbio, L. Giusti and C. Pica, Phys. Rev. Lett. **94** (2005) 032003 [arXiv:hep-th/0407052].
26. W. M. Yao *et al.* [Particle Data Group], J. Phys. G **33** (2006) 1.
27. M. A. Shifman, A. I. Vainshtein and V. I. Zakharov, Phys. Lett. B **76** (1978) 471.
28. R. Alkofer, M. A. Nowak, J. J. M. Verbaarschot and I. Zahed, Phys. Lett. B **233** (1989) 205.
29. T. Feldmann, P. Kroll and B. Stech, Phys. Rev. D **58** (1998) 114006 [arXiv:hep-ph/9802409]; T. Feldmann, P. Kroll and B. Stech, Phys. Lett. B **449** (1999) 339 [arXiv:hep-ph/9812269].
30. D. Klabucar and D. Kekez, Phys. Rev. D **58** (1998) 096003 [arXiv:hep-ph/9710206].
31. C. S. Fischer and R. Alkofer, Phys. Rev. D **67**, 094020 (2003) [arXiv:hep-ph/0301094].
32. R. Alkofer, W. Detmold, C. S. Fischer and P. Maris, Phys. Rev. D **70** (2004) 014014 [arXiv:hep-ph/0309077]; Nucl. Phys. Proc. Suppl. **141** (2005) 122 [arXiv:hep-ph/0309078].
33. S. L. Adler, Phys. Rev. **177** (1969) 2426; S. L. Adler and W. A. Bardeen, Phys. Rev. **182** (1969) 1517; J. S. Bell and R. Jackiw, Nuovo Cim. A **60** (1969) 47.
34. S. Narison, Nucl. Phys. B **509** (1998) 312 [arXiv:hep-ph/9612457].
35. O. Lakhina and P. Bicudo, arXiv:0708.0984 [hep-ph].
36. C. D. Roberts and A. G. Williams, Prog. Part. Nucl. Phys. **33**, 477 (1994) [arXiv:hep-ph/9403224].
37. R. Alkofer and L. von Smekal, Phys. Rept. **353**, 281 (2001) [arXiv:hep-ph/0007355].
38. P. Maris and C. D. Roberts, Int. J. Mod. Phys. **E12**, 297 (2003) [arXiv:nucl-th/0301049].
39. C. S. Fischer, J. Phys. **G32** (2006) R253 [arXiv:hep-ph/0605173].
40. R. Alkofer, C. S. Fischer and F. J. Llanes-Estrada, Mod. Phys. Lett. A **23** (2008) 1105 [arXiv:hep-ph/0607293].
41. M.R. Frank, K.L. Mitchell, C.D. Roberts and P.C. Tandy, Phys. Lett. B **359** (1995) 17 [arXiv:hep-ph/9412219].
42. R. Alkofer and C. D. Roberts, Phys. Lett. B **369** (1996) 101 [arXiv:hep-ph/9510284].
43. M. S. Bhagwat, L. Chang, Y. X. Liu, C. D. Roberts and P. C. Tandy, Phys. Rev. C **76** (2007) 045203 [arXiv:0708.1118 [nucl-th]].
44. D. Zwanziger, Phys. Rev. D **65** (2002) 094039 [arXiv:hep-th/0109224].
45. E. M. Ilgenfritz, P. Gerhold, M. Muller-Preussker, B. V. Martemyanov and A. I. Veselov, PoS **LAT2005** (2006) 306 [arXiv:hep-lat/0509171].
46. E. M. Ilgenfritz, M. Muller-Preussker and D. Peschka, Phys. Rev. D **71** (2005) 116003 [arXiv:hep-lat/0503020].
47. C. Gatttringer, Phys. Rev. D **67** (2003) 034507 [arXiv:hep-lat/0210001].
48. T. C. Kraan and P. van Baal, Nucl. Phys. B **533** (1998) 627 [arXiv:hep-th/9805168].
49. K. M. Lee and C. h. Lu, Phys. Rev. D **58** (1998) 025011 [arXiv:hep-th/9802108].
50. J. Greensite, Eur. J. Phys. **ST140** (2007) 1; Prog. Part. Nucl. Phys. **51** (2003) 1 [arXiv:hep-lat/0301023].
51. R. Bertle, M. Engelhardt and M. Faber, Phys. Rev. D **64** (2001) 074504 [arXiv:hep-lat/0104004].
52. R. Alkofer and J. Greensite, J. Phys. G **34**, S3 (2007) [arXiv:hep-ph/0610365].
53. J. Gattnar, K. Langfeld and H. Reinhardt, Phys. Rev. Lett. **93** (2004) 061601 [arXiv:hep-lat/0403011].